Investigational New Drugs (2019) 37:771–778
https://doi.org/10.1007/s10637-018-0711-9

SHORT REPORT

Cyclodextrin polymers decorated with RGD peptide as delivery systems for targeted anti-cancer chemotherapy

Maurizio Viale[1] · Rita Tosto[2] · Valentina Giglio[3] · Giuseppe Pappalardo[2] · Valentina Oliveri[3] · Irena Maric[1] · Maria Addolorata Mariggiò[4] · Graziella Vecchio[3]

Received: 10 November 2018 / Accepted: 5 December 2018 / Published online: 17 December 2018

Summary

Polymeric cyclodextrin–based nanoparticles are currently undergoing clinical trials as nanotherapeutics. Using a non-covalent approach, we decorated two cross-linked cyclodextrin polymers of different molecular weights with an RGD peptide derivative to construct a novel carrier for the targeted delivery of doxorubicin. RGD is the binding sequence for the integrin receptor family that is highly expressed in tumour tissues. The assembled host–guest systems were investigated using NMR and DLS techniques. We found that, in comparison with free doxorubicin or the binary complex doxorubicin/cyclodextrin polymer, the RGD units decorating the cyclodextrin-based nanosystems improved the selectivity and cytotoxicity of the complexed doxorubicin towards cultured human tumour cell lines. Our results suggest that the nanocarriers under study may contribute to the development of new platforms for cancer therapy.

Keywords Carbohydrates · Peptides · Nanoparticles · Cancer · Doxorubicin

Introduction

In the past few years, nanoparticles (NPs) have drawn interest as potential drug delivery systems that may selectively accumulate in tumour tissues, exploiting the EPR (enhanced permeability retention) effect [1].

There have been numerous studies on NPs functionalized with fluorophores, peptides, vitamins, cell adhesion molecules, aptamers, or other biomolecules for targeting specific tissues, thereby representing great promise for imaging and drug delivery [2–6].

Cyclodextrins (CyDs), cyclic oligomers of α-1,4-linked D(+)-glucopyranose, can form NPs by self-aggregation [7, 8], but the NPs often have low physical stability and their applicability is limited, especially as drug delivery systems [9]. Therefore, there is great interest in the development of stable NPs based on polymeric CyDs [10–13]. The functionalization of CyDs with molecules that have different properties provides a powerful approach to the building of multifunctional materials [11, 14].

A variety of polymeric CyDs has been synthesized: covalently cross-linked, linear, or branched polymers [15]. Epichlorohydrin (EPI) has often been used to synthesize cross-linked, water-soluble CyD polymers as drug nanocarriers [16, 17]. Cross-linked CyD polymers have been evaluated for drug delivery applications [16]. More recently, CyD oligomer synthesis has also been reported [18, 19], as low–molecular weight drug carriers have such advantages as easy excretion by renal tubules without degradation [20]. Furthermore, the inclusion of guest molecules with CyD oligomers appears to be more effective [17, 18, 21]. We have found that β-CyD and amino-β-CyD oligomers can interact with fibrin gels, resulting in controlled drug release [17].

✉ Giuseppe Pappalardo
Giuseppe.pappalardo@cnr.it

✉ Graziella Vecchio
Gr.vecchio@unict.it

[1] IRCCS Ospedale Policlinico San Martino, U.O.C. Bioterapie, L.go R. Benzi 10, 16132 Genoa, Italy

[2] CNR Istituto di Biostrutture e Bioimmagini, Sede di Catania, Via Paolo Gaifami 18, 95126 Catania, Italy

[3] Dipartimento di Scienze Chimiche, Università degli Studi di Catania, Viale A. Doria 6, 95125 Catania, Italy

[4] Dipartimento di Scienze Biomediche ed Oncologia Umana, Università degli Studi di Bari Aldo Moro, Piazza G. Cesare 11, 70124 Bari, Italy

Advanced systems may be obtained by adding recognition units to the CyD polymers. However, there are few reported examples where targeting moieties are incorporated into the CyD polymer–based nanocarrier. One example is CALAA-01, a gene delivery system that contains transferrin as the target unit [22]. In other cases, folic acid has been conjugated as the targeting ligand for selective delivery of CyD NPs to cancer cells [23, 24].

In this regard, supramolecular host–guest chemistry can be used advantageously to decorate CyD-based NPs with high recognition motif specificity [25]. Toward this goal, particular attention should be focused on the chemical synthesis of novel bioactive peptides conjugated with guest moieties fitting the CyD cavity, studies of their inclusion complexes as well as the interaction of the whole delivery system with specific targets.

Based on this interest, we report here our investigation of NPs based on β-CyD polymers targeted with, RGD (arginylglycylaspartic acid) peptide as nanocarriers of doxorubicin (dox), one of the most potent anthracycline anti-cancer drugs. Many carriers have been developed to optimize dox administration, such as liposomal Caelyx/Doxil and Myocet [26]. CyD nanoassemblies have also shown great potential for improving the pharmacological profile of dox [27]. The development of new targeted carriers is of interest [28] for reducing severe dox cardiotoxicity and improving its uptake [29].

In particular, we exploited the high affinity of the adamantyl group of the β-CyD cavity to endow CyD NPs with the RGD peptide (Fig. 1), the minimal recognition sequence for binding to the $\alpha_v\beta_3$, $\alpha_5\beta_1$ and $\alpha_v\beta_6$ integrin receptors [30]. Thus, NPs containing the RGD motif could be actively target toward integrins, which are overexpressed on tumour cell membranes, allowing selectivity between tumour and normal cells during drug delivery [31].

Here, the inclusion complexes containing the CyD polymers with dox and RGD peptides were tested in human cancer cells and compared to free dox or binary complex dox/CyD polymer.

Methods

Chemicals

All chemicals obtained from commercial sources were used without further purification. The water-soluble polymer pCyD (92 kDa, 70% CyD) was purchased from Cyclolab. (Budapest), oCyD was synthesized from β-CyD in NaOH solution with EPI as reported elsewhere [21].

The inclusion complexes were prepared by adding adamantyl–peptide conjugate (AdRGD) and dox to the CyD polymer solutions.

NMR spectroscopy

^{1}H NMR and ^{13}C NMR spectra were recorded at 25 °C with a Varian Unity Plus 500 spectrometer at 499.9 and 125.7 MHz, respectively, using standard pulse programs from the Varian library. Two-dimensional (2D) experiments (COSY [correlation spectroscopy], TOCSY [total correlation spectroscopy], HSQC [heteronuclear single quantum correlation], NOESY [nuclear Overhauser effect spectroscopy]) were acquired using 1 K data points and 256 increments. The oCyD/AdRGD (1:3 molar ratio) and pCyD/AdRGD (1:25 molar ratio) binary systems, and the oCyD/dox/AdRGD (1:2:4 molar ratio) and pCyD/dox/AdRGD (1:5:25 molar ratio) ternary systems were studied in D_2O or phosphate buffer (pD = 7.8). Spectra were referred to the D_2O signal.

Solid-phase synthesis of AdRGD

The peptide chain was assembled on a Novabiochem TGR resin (substitution 0.22 mmol/g in 0.1 mmol scale) using the Fmoc ([(9-fluorenylmethyl) oxy] carbonyl)/tert-butyl chemical approach. All Fmoc amino acids were introduced using 1-cyano-2-ethoxy-2-oxoethylidenaminooxy)dimethylamino-morpholino-carbenium hexafluorophosphate (COMU) as a coupling reagent. 15-(9-Fluorenylmethyloxycarbonyl)amino-4,7,10,13-tetraoxa-pentadecanoic acid (PEG_4) and 1-adamantane carboxylic acid were linked to the peptidyl resin using a standard double coupling instrumental protocol of a CEM Liberty peptide synthesizer. The following instrument conditions were used for each coupling cycle: microwave power, 25 W; reaction temperature, 75 °C; coupling time, 300 s. The instrumental conditions used for the deprotection cycle were: microwave power, 25 W; reaction temperature, 75 °C; deprotection time, 180 s. Fmoc group removal during synthesis was achieved using 20% piperidine solution in DMF (N,N-dimethylformamide).

AdRGD was cleaved from the resin with a mixture of TFA (trifluoroacetic acid)/TIS (triisopropylsilane)/H_2O (95:2.5:2.5), concentrated in vacuo and precipitated with freshly distilled diethyl ether. The peptide purity was checked by analytical HPLC (high-performance liquid chromatography) using a bio-basic C18 column and according to the following instrument conditions: linear gradient from 10% to 30% (eluent A: water containing 0.1% TFA, eluent B: CH_3CN containing 0.1 TFA) in 25 min; flow rate, 300 μl/min; retention time, 20 min. AdRGD identity was confirmed by electrospray ionisation mass spectrometry (ESI-MS) [m/z calculated for $C_{36}H_{62}N_8O_{12}$, 798.92; observed, 799.81 (MH^+)].

^{1}H NMR (D_2O, 500 MHz) δ (ppm): 4.52 (m, 1H, α of D); 4.24 (m, 1H, α of R); 3.86 (m, 2H, CH_2 G); 3.69 (m, 2H, c of PEG); 3.60 (m, 16H, PEG); 3.51 (t, 2H, J = 5.41 Hz, b of PEG), 3.30 (t, 2H, J = 5.40 Hz, a of PEG), 3.12 (t, 2H, J = 6.91 Hz, δ of R); 2.85 (dd, H, J = 5.42, 17.34 Hz, β of D); 2.77

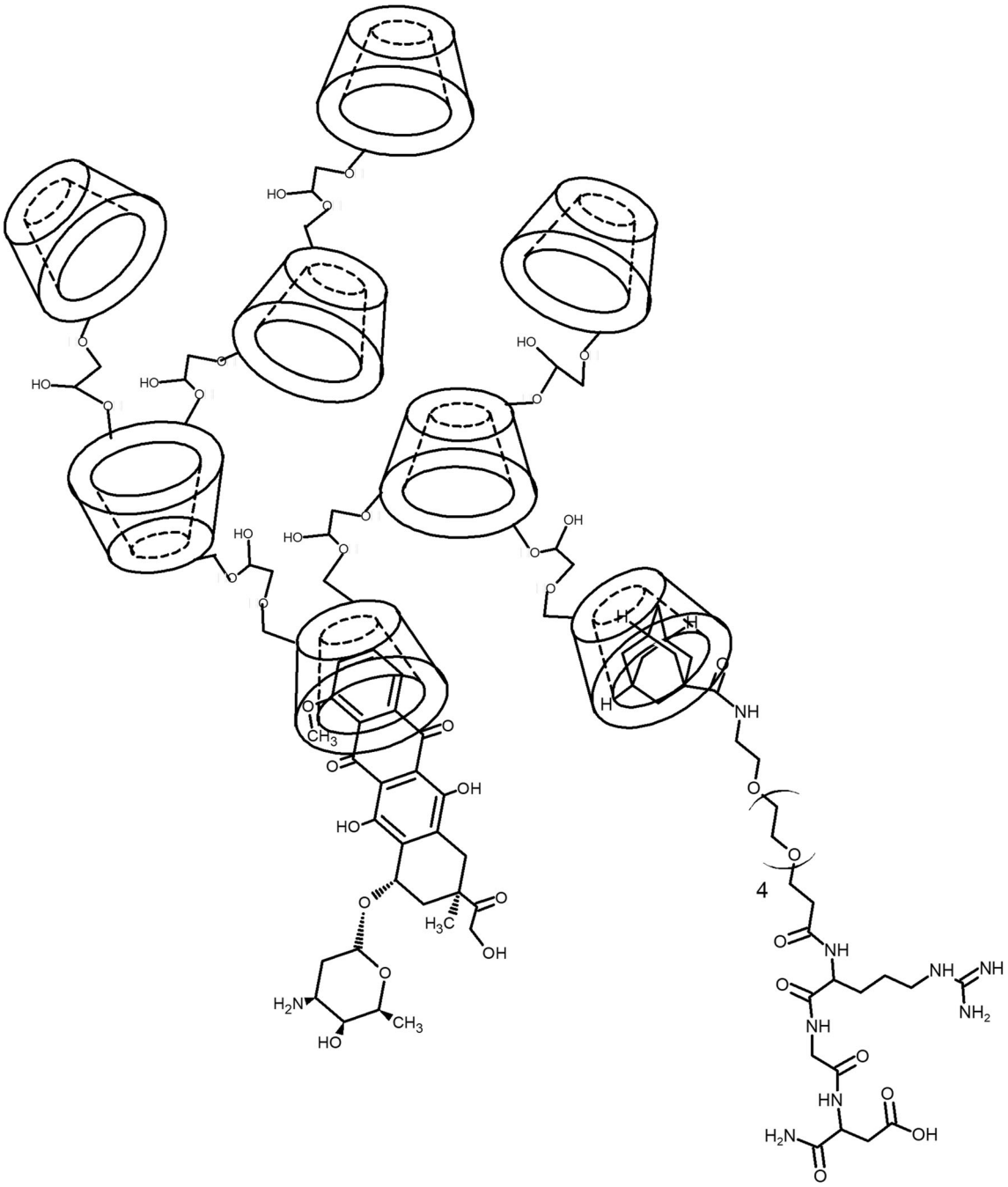

Fig. 1 Schematic representation of the oCyD, AdRGD and Dox assembly. For the sake of clarity only two occupied cavities are shown

(dd, H, $J = 7.77$, 17.34 Hz, β' of D); 2.51 (m, 2H, d of PEG); 1.92 (s, 3H, H-3, −5, −7 of Ad); 1.78 (m, 1H, β' of R); 1.75–1.46 (m, 15H, γ of R, other Hs of Ad).

^{13}C NMR (D_2O, 125 MHz) δ (ppm): 182.2 (COOH); 174–175.5 (CONH) 170.5 (CONH of Ad) 156.5 (C=NH); 69.2–69.0 (CH_2 PEG); 68.6 (Cb); 66.5 (Cc); 53.2 (Cα of R); 42.0 (CH_2 of G); 40.3 (Cδ of R); 38.7 (Ca); 38.1 (C-2, −3, −8 of Ad); 35.5 (Cγ of R); 35.4 (Cd); 35.2 (Cβ of D); 27.7 (Cβ of R); 27.4 (C-3, −5, −7 of Ad); 24.1 (C-4, −5, −6 of Ad).

Dynamic light scattering

Dynamic light scattering (DLS) measurements were performed at 25 °C with a Zetasizer Nano ZS (Malvern Instruments, UK) operating at 633 nm (He–Ne laser). The mean hydrodynamic diameter (d) of the NPs was calculated from intensity measurements. The oCyD/AdRGD and pCyD/AdRGD binary complexes were studied at the molar ratios of 1:1 to 20. The oCyD/dox/AdRGD/ and pCyD/dox/AdRGD/

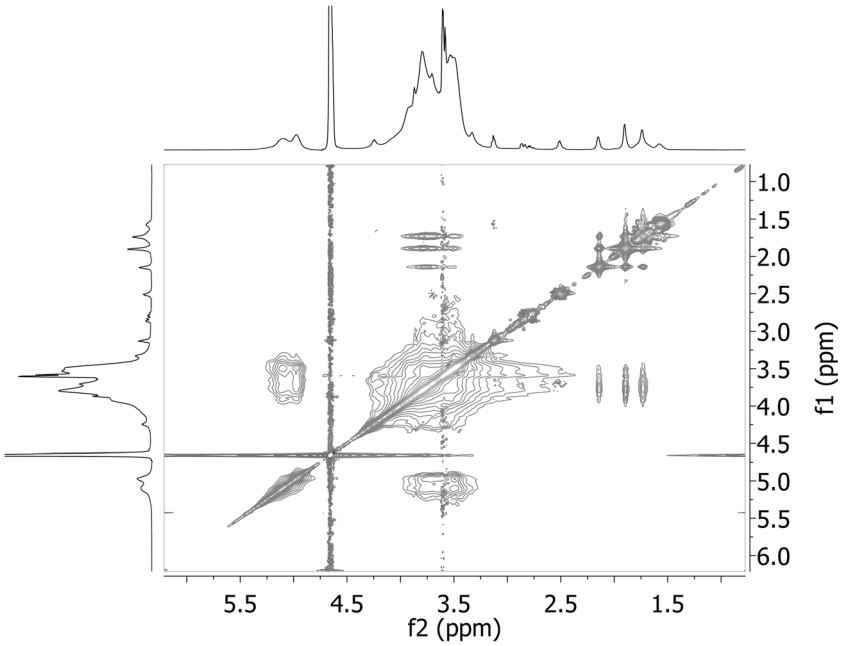

Fig. 2 NOESY spectrum of pCyD/AdRGD complex (D_2O, 500 MHz)

ternary complexes were studied at the molar ratios of 1:2:4: and 1:5:20:, respectively. The samples were diluted in phosphate buffer (pH = 7.4).

Tetrazolium (MTT) assay evaluation of antiproliferative activity

The human cancer cell lines A2780 (ovary adenocarcinoma), A549 (lung carcinoma), MDA-MB-231 (breast carcinoma) and SH-SY5Y (neuroblastoma) were plated in flat-bottom 96-well microtiter plates at densities of 1600–3600 per well. After 6–8 h, the cells were treated with 20 μl containing five 1:5 fold concentrations of dox loaded in CyD polymers (starting from 1 μM) diluted in normal saline. The plates were then processed as described elsewhere [32]. oCyD or pCyD complexes containing AdRGD concentrations at AdRGD/dox ratios of 2:1 to 40:1 were assayed.

The concentrations inhibiting 50% of cell growth (IC_{50}) were calculated based on concentration–response curve analysis. Each experiment was repeated 4–11 times.

Table 1 IC_{50} (nM) values of dox and its complexes with oCyD or pCyD in A2780, A549, MDA-MB-231 and SH-SY5Y cells

Compounds	Cell lines			
	A2780	A549	MDA-MB-231	SHSY5Y
dox	7.7 ± 3.9	54.6 ± 19.2	52.5 ± 20.0	44.3 ± 9.4
oCyD-dox	13.2 ± 3.9[a]	80.8 ± 11.2[c]	57.8 ± 10.6	74.7 ± 19.9[e]
pCyD-dox	14.0 ± 4.8[b]	62.7 ± 15.7[d]	50.8 ± 14.4	50.1 ± 18.0[f]

The comparison between single groups was evaluated first by ANOVA, followed by the post-hoc test Fisher's protected LSD (*p*-values)

[a] $p < 0.009$ vs. dox

[b] $p < 0.003$ vs. dox

[c] $p < 0.002$ vs. dox

[d] $p < 0.030$ vs. oCyD-dox

[e] $p < 0.001$ vs. dox

[f] $p < 0.001$ vs. oCyD-dox

Statistical analysis

Statistical analysis of multiple groups was performed using one-way analysis of variance (ANOVA) followed by the post-hoc test Fisher's protected least significant difference (LSD).

Results and discussion

Synthesis and characterization

The AdRGD was obtained by linking an adamantanecarboxylic moiety to the amino terminus of the RGD peptide through a PEG_4 chain. The synthesized RGD peptide was C-terminally protected as an amide to remove unwanted end charge. The AdRGD product was characterized with ESI-MS and NMR. AdRGD was used to exploit the host–guest interaction between CyD and adamantane and introduce targeting units in the CyD-based NPs.

The inclusion complexes of pCyD or oCyD with AdRGD and dox were characterized using NMR spectroscopy in D_2O and in phosphate buffer (D_2O, pD = 7.8).

Table 2 IC_{50} (nM) values of dox with CyD polymers and AdRDG in human tumour cells

	oCyD-dox	AdRGD 1X	AdRGD 2X	AdRGD 4X	AdRGD 8X	AdRGD 20X	AdRGD 40X	*pCyD-dox*	AdRGD 1X	AdRGD 2X
A2780	13.2 ± 3.9	13.0 ± 2.2	15.4 ± 6.6	10.0 ± 4.2	6.5 ± 2.2	9.4 ± 4.4	12.8 ± 3.4	14.0 ± 4.8	12.9 ± 2.1	13.7 ± 5.7
A549	80.8 ± 11.2	76.9 ± 13.3	68.8 ± 23.3	68.4 ± 14.2	49.1 ± 5.3	44.9 ± 8.8	51.3 ± 16.2	62.7 ± 15.7	52.3 ± 15.9	63.2 ± 14.7
MDA-MB-231	57.8 ± 10.6	56.6 ± 10.3	47.0 ± 9.9	41.3 ± 11.2	57.8 ± 7.8	63.5 ± 7.1		50.8 ± 14.4	41.6 ± 13.5	50.7 ± 14.0
SHSY5Y	74.7 ± 19.9	71.1 ± 13.7	38.2 ± 5.6	30.6 ± 10.6	47.7 ± 22.1	63.0 ± 19.0	65.3 ± 18.8	50.1 ± 18.0	55.7 ± 13.4	41.4 ± 5.8

	AdRGD 4X	AdRGD 8X	AdRGD 20X	AdRGD 40X	*Dox*	AdRGD 4X	AdRGD 8X	AdRGD 20X
A2780	8.7 ± 3.4	5.9 ± 1.4	7.8 ± 2.1	12.7 ± 2.8	7.7 ± 3.9	7.9 ± 1.4	6.1 ± 0.7	11.6 ± 2.9
A549	66.8 ± 11.4	46.3 ± 14.9	55.4 ± 18.9		54.6 ± 19.2	56.9 ± 6.5	51.2 ± 22.5	49.3 ± 22.5
MDA-MB-231	32.4 ± 5.6	50.7 ± 15.2	47.4 ± 9.8		52.5 ± 20.0	50.3 ± 22.1	69.2 ± 7.7	49.5 ± 10.2
SHSY5Y	40.8 ± 9.7	43.5 ± 11.2	46.1 ± 11.1	56.8 ± 15.7	44.3 ± 9.4	41.4 ± 13.3	48.16 ± 5.2	47.2 ± 6.1

In the ^{1}H NMR spectra of pCyD with AdRGD, all AdRGD proton signals were broadened in keeping with the formation of the inclusion complex. The Ad proton signals were downfield-shifted in the spectra compared to that of free AdRGD. In the NOESY spectrum (Fig. 2), the signals due to adamantane residue showed NOE correlations with the H-5 and H-6 protons of the CyDs, further suggesting the inclusion of the Ad residue.

The ternary complexes of oCyD or pCyD with dox and AdRGD were characterized using NMR. The ^{1}H NMR spectrum showed broadening of the dox proton signals, which suggested the interaction of dox with the polymers. We also performed NOESY experiments of the ternary systems. The spectra showed many NOE correlations due to dox protons, which partially overlapped the CyD proton signals. Dox did not replace the included AdRGD, whose protons showed strong correlations with the CyD protons in the ternary complex spectra.

DLS measurements

The binary (polymer/AdRGD) and ternary (polymer/dox/AdRGD) systems were studied using DLS at pH 7.4 (phosphate buffer) and compared to the parent systems. The AdRGD-alone particle size distribution showed that AdRGD formed different NP populations with a hydrodynamic diameter (d) of 24 nm and 200 nm, respectively, as found for similar systems [33]. The CyD polymers formed NPs with d = 5.1 nm (oCyD) and d = 23 nm (pCyD). When oCyD was added to AdRGD, a main NP population of 6.2 nm was detected.

The pCyD NP size increased slightly (25 nm) upon the addition of AdRGD, but the addition of dox did not modify the NP size.

Antiproliferative activity of AdRGD-polymer complexes

We performed cell proliferation assays on dox-sensitive human cancer cell lines, i.e. ovarian carcinoma A2780, lung adenocarcinoma A549, breast carcinoma MDA-MB-231 and neuroblastoma SH-SY5Y (Tables 1 and 2).

Table 1 shows that the complexes did not have higher antiproliferative activity than dox for any case, as typically found for similar systems [17, 34, 35]. Furthermore, pCyD-dox showed better activity than oCyD-dox in A549 ($p = 0.03$) and SH-SY5Y cells ($p = 0.001$).

When the complexes were mixed with AdRGD, the antiproliferative activity varied with the ratio between the concentrations of AdRGD and dox (Table 2).

In particular, the effect of AdRGD was more significant when mixed with oCyD-dox (Fig. 3) in A549 cells at ratios of 8X ($p = 0.001$), 20X ($p = 0.001$) and 40X ($p = 0.001$) in

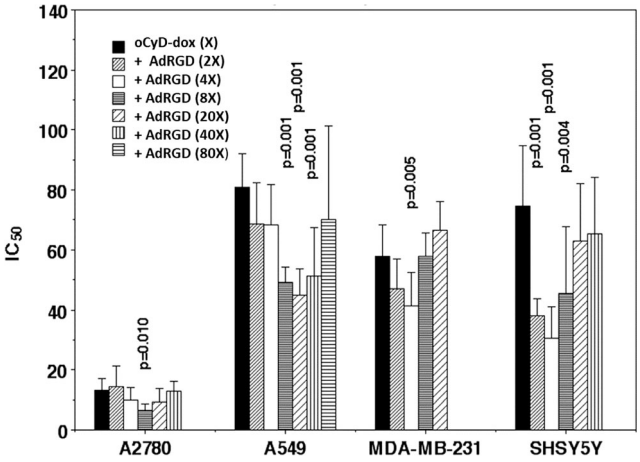

Fig. 3 IC_{50} (nM) of oCyD-dox alone or with AdRGD in human cancer cell lines

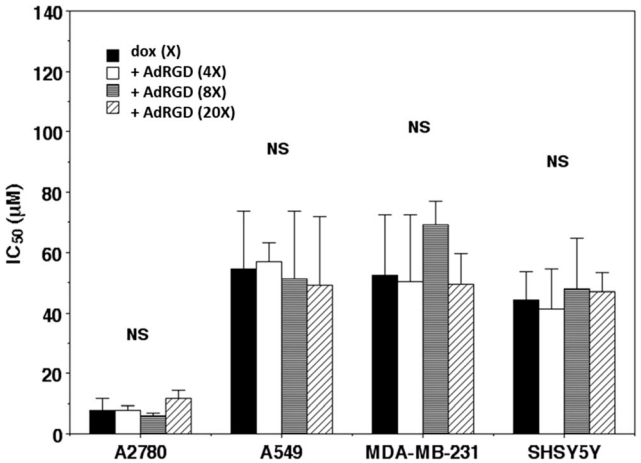

Fig. 5 IC_{50} (nM) of dox alone or with AdRGD in human cancer cell lines

MDA-MB-231 cells at a ratio of 4X ($p = 0.005$) and in SH-SY5Y cells at ratios of 2X ($p = 0.001$), 4X ($p = 0.001$) and 8X ($p = 0.004$). Finally, in A2780 cells, the addition of AdRGD at the ratio 8X caused clear enhancement of dox antiproliferative activity as compared to the oCyD-dox complex ($p < 0.01$) (Fig. 3).

The increase of the antiproliferative activity for AdRGD with pCyD-dox was evident only in the A2780 cells at the ratios of 4X ($p = 0.010$), 8X ($p = 0.001$) and 20X ($p = 0.006$), and in MDA-MB-231 cells at the ratio of 4X ($p < 0.016$) (Fig. 4).

It is important to note that AdRGD did not show antiproliferative activity (data not shown) when administered alone, and that at the doses used, AdRGD did not potentiate free dox activity in any cases (Fig. 5).

Clearly, the addition of AdRGD generally potentiated the antiproliferative activity of dox in both CyD polymers but only for specific concentration ratios. This effect was greater when AdRGD was combined with the oCyD-dox binary complex.

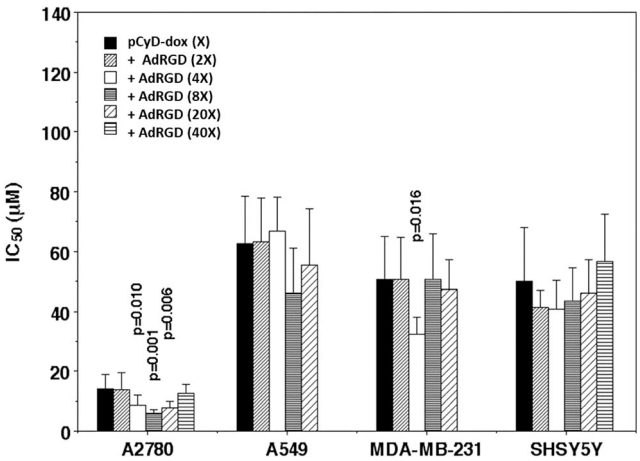

Fig. 4 IC_{50} (nM) of pCyD-dox alone or with AdRGD in human cancer cell lines

The different activity observed for the defined AdRGD/dox ratios could be related to two pharmacodynamic causes. The first is the different cell expression of integrins: only a subset of which can recognize AdRGD and initiate the process of targeting dox-CyD polymers. Indeed, as reported above, the tripeptide RGD sequence, found in many extracellular matrix proteins, is a promiscuous binder of integrins and has been widely used to address drugs and probes to tumours [7]. The tested cell lines express different levels of the various integrin family members [36]. In particular, MDA-MB-231 cells express low levels of $\alpha_v\beta_3$ and $\alpha_v\beta_6$ integrins, whereas the A549 cells express high levels of $\alpha_v\beta_5$ and no $\alpha_v\beta_6$. Interestingly, A2780 cells do not express any $\alpha_v\beta_3$ receptors, but $\alpha_v\beta_5$ receptors are present on A2780 cell surfaces. Finally, SH-SY5Y cells express high levels of several integrin family members, including many α and β subunits as well as the $\alpha_v\beta_3$ receptor [37]. In these conditions and at specific AdRGD concentrations, the tumour cells showed different sensitivity to dox.

Conclusions

We describe a convenient supramolecular strategy for constructing nanocarriers based on CyD polymers endowed with recognition elements for targeted delivery. Two β-CyD–EPI cross-linked polymers of different molecular weights were decorated with AdRGD to target tumour cells. All of the supramolecular systems included the anti-cancer agent dox, and affected its antiproliferative activity.

The pCyD/AdRGD and oCyD/AdRGD supramolecular complexes were able to increase the cytotoxicity of dox significantly, and this ability depended on the dimension of the nanocarrier and the amount of target unit. Overall, there was no change in the anti-cancer activity of the complex of dox with the high–molecular weight CyD polymer (pCyD) compared to free dox, and it was less influenced by the presence of

AdRGD. The oCyD/dox/AdRGD ternary complex showed increased cytotoxicity of up to two times greater than that of the oCyD/dox binary complexes in the A2780 and SH-SY5Y cell lines. The experimental evidence reported in this paper proves how powerful low–molecular weight CyD polymers (oCyD) are as tools for forming macromolecular architectures devoted to targeted drug delivery.

Acknowledgments The authors are grateful for support from Università degli Studi di Catania (Piano della Ricerca di Ateneo 2016-2018) and the Italian Ministero dell'Università e della Ricerca. Training grant PO FSE 2014-2020 (Tosto R.) is also gratefully acknowledged.

Funding This study was funded by Università degli Studi di Catania (Piano della Ricerca di Ateneo 2016-2018) and PO FSE 2014-2020 (MIUR).

Compliance with ethical standards

Ethical approval This article does not contain any studies with human participants or animals performed by any of the authors.

Conflict of interest All the authors declare that they have no conflict of interest.

Informed consent For this type of study, formal consent is not required.

References

1. Maeda H (2015) Toward a full understanding of the EPR effect in primary and metastatic tumors as well as issues related to its heterogeneity. Adv Drug Deliv Rev 91:3–6. https://doi.org/10.1016/j.addr.2015.01.002
2. Gallego-Yerga L, Benito JM, Blanco-Fernández L et al (2018) Plasmid-templated control of DNA–cyclodextrin nanoparticle morphology through molecular vector design for effective gene delivery. Chem Eur J 24:3825–3835. https://doi.org/10.1002/chem.201705723
3. Chinen AB, Guan CM, Ferrer JR et al (2015) Nanoparticle probes for the detection of cancer biomarkers, cells, and tissues by fluorescence. Chem Rev 115:10530–10574. https://doi.org/10.1021/acs.chemrev.5b00321
4. Spicer CD, Jumeaux C, Gupta B, Stevens MM (2018) Peptide and protein nanoparticle conjugates: versatile platforms for biomedical applications. Chem Soc Rev 47:3574–3620. https://doi.org/10.1039/c7cs00877e
5. Velpurisiva P, Gad A, Piel B et al (2017) Nanoparticle design strategies for effective cancer immunotherapy. J Biomed 2:64–77. https://doi.org/10.7150/jbm.18877
6. Xiao Z, Levy-Nissenbaum E, Alexis F et al (2012) Engineering of targeted nanoparticles for cancer therapy using internalizing aptamers isolated by cell-uptake selection. ACS Nano 6:696–704. https://doi.org/10.1021/nn204165v
7. Danhier F, Le BA, Préat V (2012) RGD-based strategies to target alpha(v) beta(3) integrin in cancer therapy and diagnosis. Mol Pharm 9:2961–2973. https://doi.org/10.1021/mp3002733
8. Zhu X, Xiao S, Zhou D et al (2018) Design, synthesis and biological evaluation of water-soluble per-O-methylated cyclodextrin-C60 conjugates as anti-influenza virus agents. Eur J Med Chem 146:194–205. https://doi.org/10.1016/j.ejmech.2018.01.040
9. Bonnet V, Gervaise C, Djedaïni-Pilard F et al (2015) Cyclodextrin nanoassemblies: a promising tool for drug delivery. Drug Discov Today 20:1120–1126
10. Wang J, Sun J, Chen Q et al (2012) Star-shape copolymer of lysine-linked di-tocopherol polyethylene glycol 2000 succinate for doxorubicin delivery with reversal of multidrug resistance. Biomaterials 33:6877–6888. https://doi.org/10.1016/j.biomaterials.2012.06.019
11. De Barros SDT, Senra JD, Tinoco LW et al (2016) Characterization of a ternary system based on hybrid nanoparticles. J Nanosci Nanotechnol 16:2822–2831. https://doi.org/10.1166/jnn.2016.11771
12. Mejia-Ariza R, Graña-Suárez L, Verboom W, Huskens J (2017) Cyclodextrin-based supramolecular nanoparticles for biomedical applications. J Mater Chem B 5:36–52
13. Caldera F, Tannous M, Cavalli R et al (2017) Evolution of cyclodextrin nanosponges. Int J Pharm 531:470–479. https://doi.org/10.1016/j.ijpharm.2017.06.072
14. Cutrone G, Casas-Solvas JM, Vargas-Berenguel A (2017) Cyclodextrin-modified inorganic materials for the construction of nanocarriers. Int J Pharm 531:621–639. https://doi.org/10.1016/j.ijpharm.2017.06.080
15. Oliveri V, Vecchio G (2018) Cyclodextrin-based nanoparticles in Organic materials as smart nanocarriers for drug delivery, pp 619–658. https://doi.org/10.1016/B978-0-12-813663-8.00015-4, Elsevier 2018.
16. Gidwani B, Vyas A (2014) Synthesis, characterization and application of Epichlorohydrin-β-cyclodextrin polymer. Colloids Surf B Biointerfaces 114:130–137
17. Giglio V, Viale M, Bertone V et al (2018) Cyclodextrin polymers as nanocarriers for sorafenib. Investig New Drugs 36:370–379. https://doi.org/10.1007/s10637-017-0538-9
18. Giglio V, Sgarlata C, Vecchio G (2015) Novel amino-cyclodextrin cross-linked oligomer as efficient carrier for anionic drugs: a spectroscopic and nanocalorimetric investigation. RSC Adv 5:16664–16671. https://doi.org/10.1039/c4ra16064a
19. Anand R, Malanga M, Manet I et al (2013) Citric acid-γ-cyclodextrin crosslinked oligomers as carriers for doxorubicin delivery. Photochem Photobiol Sci 12:1841–1854. https://doi.org/10.1039/c3pp50169h
20. Longmire M, Choyke PL, Kobayashi H (2008) Clearance properties of nano-sized particles and molecules as imaging agents: considerations and caveats. Nanomedicine 3:703–717
21. Giglio V, Bellia F, Oliveri V, Vecchio G (2016) Aminocyclodextrin oligomers as protective agents of protein aggregation. Chempluschem 81:660–665. https://doi.org/10.1002/cplu.201600239
22. Davis ME, Zuckerman JE, Choi CHJ et al (2010) Evidence of RNAi in humans from systemically administered siRNA via targeted nanoparticles. Nature 464:1067–1070. https://doi.org/10.1038/nature08956
23. Liao R, Zhao Y, Liao X et al (2015) Folic acid-polyamine-β-cyclodextrin for targeted delivery of scutellarin to cancer cells. Polym Adv Technol 26:487–494. https://doi.org/10.1002/pat.3477
24. Giglio V, Viale M, Monticone M et al (2016) Cyclodextrin polymers as carriers for the platinum-based anticancer agent LA-12. RSC Adv 6:12461–12466. https://doi.org/10.1039/c5ra22398a
25. Schmidt BVKJ, Hetzer M, Ritter H, Barner-Kowollik C (2014) Complex macromolecular architecture design via cyclodextrin host/guest complexes. Prog Polym Sci 39:235–249. https://doi.org/10.1016/j.progpolymsci.2013.09.006
26. Eitan R, Fishman A, Meirovitz M et al (2014) Liposome-encapsulated doxorubicin citrate (Myocet) for treatment of recurrent epithelial ovarian cancer: a retrospective analysis. Anti-Cancer Drugs 25:101–105. https://doi.org/10.1097/CAD.0000000000000023

27. Mohammad N, Vikram Singh S, Malvi P et al (2015) Strategy to enhance efficacy of doxorubicin in solid tumor cells by methyl-β-cyclodextrin: involvement of p53 and Fas receptor ligand complex. Sci Rep 5:11853. https://doi.org/10.1038/srep11853
28. Bozzuto G, Molinari A (2015) Liposomes as nanomedical devices. Int J Nanomedicine 10:975–999
29. Sun Y, Kang C, Liu F et al (2017) RGD peptide-based target drug delivery of doxorubicin nanomedicine. Drug Dev Res 78:283–291. https://doi.org/10.1002/ddr.21399
30. Nieberler M, Reuning U, Reichart F et al (2017) Exploring the role of RGD-recognizing integrins in cancer. Cancers (Basel) 9:116. https://doi.org/10.3390/cancers9090116
31. Wang F, Li Y, Shen Y et al (2013) The functions and applications of RGD in tumor therapy and tissue engineering. Int J Mol Sci 14: 13447–13462
32. Oliveri V, Grasso GI, Bellia F et al (2015) Soluble sugar-based quinoline derivatives as new antioxidant modulators of metal-induced amyloid aggregation. Inorg Chem 54:2591–2602. https://doi.org/10.1021/ic502713f
33. Wang K, Liu Y, Li C et al (2013) Cyclodextrin-responsive micelles based on poly(ethylene glycol)-polypeptide hybrid copolymers as drug carriers. ACS Macro Lett 2:201–205. https://doi.org/10.1021/mz300568b
34. Viale M, Giglio V, Monticone M et al (2017) New doxorubicin nanocarriers based on cyclodextrins. Investig New Drugs 35:539–544. https://doi.org/10.1007/s10637-017-0461-0
35. Oliveri V, Bellia F, Viale M et al (2017) Linear polymers of β and γ cyclodextrins with a polyglutamic acid backbone as carriers for doxorubicin. Carbohydr Polym 177:355–360. https://doi.org/10.1016/j.carbpol.2017.08.103
36. Goodman SL, Grote HJ, Wilm C (2012) Matched rabbit monoclonal antibodies against v-series integrins reveal a novel v 3-LIBS epitope, and permit routine staining of archival paraffin samples of human tumors. Biol Open 1:329–340. https://doi.org/10.1242/bio.2012364
37. Ferlemann FC, Menon V, Condurat AL et al (2017) Surface marker profiling of SH-SY5Y cells enables small molecule screens identifying BMP4 as a modulator of neuroblastoma differentiation. Sci Rep 7:13612. https://doi.org/10.1038/s41598-017-13497-8